Molecular Crystals and Liquid Crystals
Publication details, including instructions for authors and subscription information:
http://www.tandfonline.com/loi/gmcl20

Ambient Smectic Ordering in Hydrogen-Bonded Liquid Crystal Homologous Series

K. Murugadass [a], V. N. Vijayakumar [a] & M. L. N. Madhu Mohan [a]
[a] Liquid Crystal Research Laboratory (LCRL), Bannari Amman Institute of Technology, Sathyamangalam, India

Version of record first published: 08 Apr 2011

To cite this article: K. Murugadass, V. N. Vijayakumar & M. L. N. Madhu Mohan (2011): Ambient Smectic Ordering in Hydrogen-Bonded Liquid Crystal Homologous Series, Molecular Crystals and Liquid Crystals, 537:1, 22-35

To link to this article: http://dx.doi.org/10.1080/15421406.2011.556418

Mol. Cryst. Liq. Cryst., Vol. 537: pp. 22–35, 2011

ISSN: 1542-1406 print/1563-5287 online
DOI: 10.1080/15421406.2011.556418

Taylor & Francis
Taylor & Francis Group

Ambient Smectic Ordering in Hydrogen-Bonded Liquid Crystal Homologous Series

K. MURUGADASS, V. N. VIJAYAKUMAR, AND M. L. N. MADHU MOHAN

Liquid Crystal Research Laboratory (LCRL), Bannari Amman Institute of Technology, Sathyamangalam, India

A homologous series of compounds with an inter-hydrogen bond formed between p-n-alkyloxy benzoic acids (nABA) and alkyl aniline were synthesized and characterized. The mesogenic p-n-alkyloxy benzoic acids (where n represents the alkyloxy carbon number from 3 to 12 except 4 and 6) formed a hydrogen bond with liquid-crystal intermediate 4-dodecyl aniline. The isolated homologous series compounds were analyzed by polarizing optical microscopy (POM), differential scanning calorimetry (DSC), Fourier transform infrared spectroscopy (FTIR), proton nuclear magnetic resonance (P-NMR), and dielectric studies. The occurrence of an ambient smectic ordering in some of the isolated mesogens was one of the interesting features of these homologous series. The phase diagrams of the p-n-alkyloxy benzoic acids and the present homologous series were computed and compared and it can be mentioned that there exists a correlation between the alkyl chain length and mesogenic phases induced. Further, some of the mesogens exhibit monotropic smectic F and smectic G transitions. The hydrogen bond formation was evinced through FTIR and P-NMR spectral studies. Results of free p-n-alkyloxy benzoic acids and the hydrogen-bonded homologous series are discussed in the light of increment alkyloxy carbon number, mesogenic phases exhibited, and mesogenic thermal range.

Keywords Benzoic acids; inter hydrogen bonding; liquid crystals; phase diagram; phase transitions; smectic phases

Introduction

Hydrogen-bonded liquid crystals have generated new interest among many research groups [1–12] due to their ease of synthesis, lower mesogenic temperatures, and fascinating properties. Discovery of H-bonded liquid crystals by Kato and Frechet [13] opened a new chapter in design, synthesis, and characterization of these mesogens. Most of the reported data [1–13] on hydrogen-bonded liquid crystals (HBLC) deal with some phase being induced. With our previous experience [14–16] in designing and synthesizing liquid crystals and in continuation of our efforts to understand hydrogen-bonded mesogens between anilines and alkyloxy benzoic acids [17], in the present work a successful attempt has been made to design and isolate a homologous

Address correspondence to M. L. N. Madhu Mohan, Liquid Crystal Research Laboratory, Bannari Amman Institute of Technology, Sathyamangalam 638 401, India. E-mail: mln.madhu@gmail.com

series of HBLC with an aim of lowering the transition temperatures of the mesogens to the ambient temperatures. The mesogenic p-n-alkyloxy benzoic acids (where n represents the alkyloxy carbon number from 5 to 12 except 4 and 6) formed a hydrogen bond with liquid-crystal intermediate 4-dodecyl aniline. Phase diagrams and mesogenic phase and thermal range are discussed for the isolated present homologous series.

Experimental

Optical textural observations were made with a Nikon polarizing microscope equipped with Nikon digital CCD camera system (Tokyo, Japan) with 5 megapixels and 2560 × 1920 pixel resolution. The liquid-crystalline textures were processed, analyzed, and stored with the aid of an ACT-2U (Tokyo, Japan) imaging software system. The temperature control of the liquid-crystal cell was equipped with an Instec HCS402-STC 200 temperature controller (Instec (Colorado, USA)) to a temperature resolution of ±0.1°C. This unit was interfaced to a computer by an IEEE–STC 200 to control and monitor the temperature. The liquid crystal sample was filled by capillary action in its isotropic state into a commercially available (Instec) polyamide buffed cell with a 5 μm spacer. The transition temperatures and corresponding enthalpy values were obtained by using differential scanning calorimetry (DSC; Shimadzu DSC-60 (Tokyo, Japan)). The Fourier transform infrared (FTIR) spectra were recorded (ABB FTIR MB3000 (Burlington, Canada)) and analyzed with the MB3000 software. Proton nuclear magnetic resonance (P-NMR) studies were done on a Bruker International model (East Milton, Canada) Ultra Shield of 300 MHz. P-NMR spectra of the compound were recorded in $CDCl_3$ with Tetra Methyl Sylene (TMS) as the internal standard. Dielectric studies were performed with an HP 4192A (Mississauga, Canada) impedance analyzer. The p-n-alkyloxy benzoic acids (nABA) and 4-dodecyl aniline were supplied by Sigma Aldrich (Munich, Germany) and all solvents used were E. Merck grade.

Synthesis of Intermolecular Hydrogen-Bonded Homologous Series

The intermolecular hydrogen-bonded compounds were synthesized by the addition of one mole of p-n-alkyloxy benzoic acids (nABA) with one mole of 4-dodecyl aniline in N,N-dimethyl formamide (DMF), respectively. They were subject to constant stirring for 12 h at ambient temperature of 30°C until a white precipitate in a dense solution was formed. The white crystalline crude compounds so obtained by removing excess DMF were then recrystallized with dimethyl sulfoxide (DMSO). The yields varied from 85 to 95% and the yield of higher homologues compounds was observed to

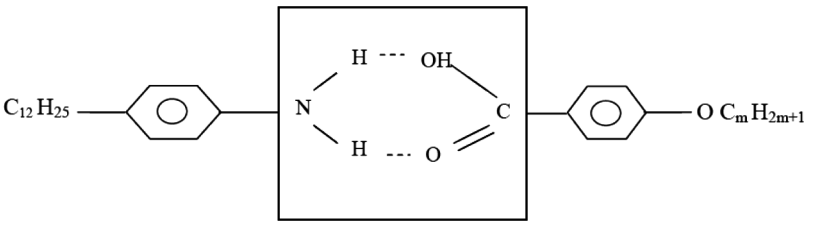

Figure 1. Molecular structure of dodecylaniline and alkyloxy benzoic acid homologous series.

be greater compared to its lower counterparts. The homologous series of p-n-alkyloxy benzoic acids with 4-dodecyl aniline can be depicted as shown in Figure 1, where m represents the alkyloxy carbon number of benzoic acid. The double hydrogen bond formation was observed between the functional group of aniline (NH_2) and the functional group of acid (COOH) of the benzoic acid, respectively.

Results and Discussion

All of the mesogens isolated under the present investigation are white crystalline solids and are stable at room temperature. They are insoluble in water and sparingly soluble in common organic solvents such as methanol, ethanol, benzene, and dicholoromethane. However, they show a high degree of solubility in coordinating solvents like DMSO, DMF, and pyridine. All of these mesogens melt at specific temperatures below 150°C (Table 1). They show high thermal and chemical stability when subjected to repeat thermal scans performed during thermal microscopy, DSC, and dielectric studies.

Infrared Spectroscopy and P-NMR Studies

The Infrared (IR) spectra of p-n-alkyloxy benzoic acid, 4-dodecyl aniline, and their intermolecular H-bonded compound were recorded in the solid state (KBr) at room temperature. Figure 2a illustrates the FTIR spectra of octyl benzoic acid and dodecyl aniline hydrogen-bonded compounds. The solid-state spectra of free alkyloxy benzoic acid is reported [18] to have two sharp bands at 1685 and 1695 cm^{-1} due to the frequency ν(C=O) mode. The doubling feature of this stretching mode confirms the dimeric nature of alkyloxy benzoic acid at room temperature [19]. As seen in Figure 2a, a strong intense band appearing at 2916 cm^{-1} is assigned to the ν(O-H) mode of the carboxylic acid group. The IR spectra (KBr) of 4-dodecyl aniline shows characteristic bands for ν(N-H) ($\sim$3371 cm^{-1}) and ν(C-O) ($\sim$1257 cm^{-1}) stretching modes. The hypsochromic shift in ν(C=O) of acid ($\sim$62 cm^{-1}) and bathochromic shift in the ν(OH) ($\sim$8 cm^{-1}) mode of acid in the present series suggest the formation of intermolecular H-bonding between the –COOH group of p-n-alkyloxy benzoic acids and the –NH of 4-dodecyl aniline. The presence of H-bonding in the present compounds was further inferred by the appearance of new band diagnostic of $\nu(O \cdots H)$ at 2581 cm^{-1}.

The proposed structure of 12A+nBA compounds has been verified by P-NMR studies. As a representative case, ^{1}H NMR for the 12A+8BA compound is discussed. The compounds were analyzed using nuclear magnetic resonance (NMR) spectroscopy (Bruker International). NMR spectra of the compound were recorded in $CDCl_3$ with TMS as the internal standard. The recorded spectrum is shown in Figure 2b and the following chemical shifts were observed.

(a) Broad resonance signals are observed approximately in the range of 0.5–2.8 ppm for the methylene group. In 12A+8BA compound these signals are observed between 2.511 and 0.867 ppm, which is attributed to the existence of the tacticity of the backbone methylene.
(b) Two sets of multiplets between 6.983 and 6.619 ppm and 8.093 and 8.035 ppm are equivalent to 2H and are attributed to aromatic protons.
(c) The existence of the amine group is identified by the appearance of a peak at 4.0 ppm.

Table 1. Transition temperatures obtained by DSC of 12A+nBA homologous series

Carbon number	Phase variant	Technique	Crystal to melt	N	C	F	G	Crystal
3	G	DSC (h)	53.2 (85.76)				96.9 (0.46)	
		DSC (c)					103.4 (3.31)	95.4 (14.15)
5	G	DSC (h)	[a]				[b]	[a]
		DSC (c)					58.6 (0.20)	
7	FG	DSC (h)	[a]			79.2 (5.93)	54.0 (9.21)	[a]
		DSC (c)				103.6 (12.38)	75.5 (7.11)	
8	FG	DSC (h)	74.4 (15.14)			82.4 (0.29)	[b]	
		DSC (c)				80.6 (2.38)	46.7 (merged with crystal)	45.4 (21.33)
9	NCF	DSC (h)	94.2 (108.27)	141.8 (3.36)	116.2 (3.93)	[b]		
		DSC (c)		138.5 (3.10)	112.6 (2.14)	89.6 (28.76)		66.8 (71.07)
10	FG	DSC (h)	87.0 (12.69)			102.0 (8.40)	87.0 (14.71)	
		DSC (c)				104.3 (3.45)	83.6 (8.61)	73.5 (10.14)
11	CFG	DSC (h)	96.2 (53.13)		87.9 (3.81)	Merged with C	[b]	
		DSC (c)			102.4 (not resolved)	81.6 (2.96)	79.5 (1.00)	74.8 (51.22)
12	CFG	DSC (h)	93.7 (38.88)		102.8 (1.91)	93.7 (38.88)	[b]	
		DSC (c)			97.8 (2.23)	82.4 (11.68)	63.2 (9.47)	43.9 (7.95)

[a]Room-temperature liquid crystal.
[b]Monotropic transition.

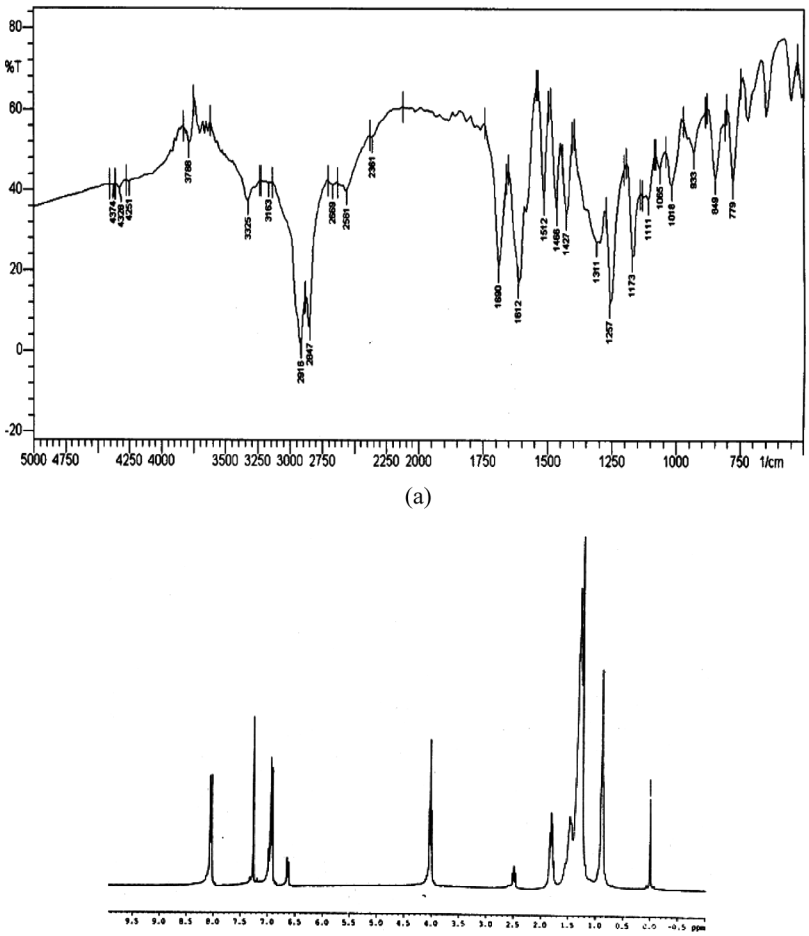

Figure 2. (a) FTIR spectrum of 12A+8BA. (b) Proton NMR spectra of 12A+8BA.

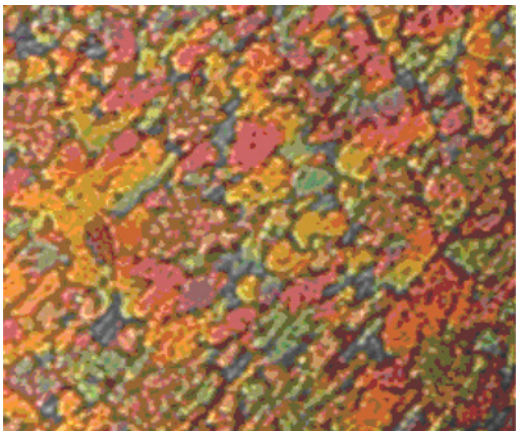

Figure 3. Checkerboard texture of the smectic F phase.

Phase Identification

The observed phase variants, transition temperatures, and corresponding enthalpy values obtained by DSC in cooling and heating runs for both homologous series are presented in Table 1. The phase diagram is constructed from the data obtained from the cooling run of DSC.

Dodecyl Aniline and Benzoic Acids Homologous Series

Dodecyl aniline and benzoic acid homologous series compounds, on cooling from isotropic melt, are found to exhibit characteristic textures [20], viz. nematic (threaded nematic), smectic C (Schlieren) smectic F (checkerboard texture), and smectic G (smooth, multicolored mosaic texture). Figures 3 and 4 represent smectic F and smectic G phases, respectively. The general phase sequence of the dodecyl aniline and benzoic acid homologous series in the cooling run can be shown as:

Isotropic → Sm G → Crystal	(compound with carbon numbers 3 and 5)
Isotropic → Sm F → Sm G → Crystal	(compound with carbon numbers 7, 8, and 10)
Isotropic → N → Sm C → Sm F → Crystal	(compound with carbon number 9)
Isotropic → Sm C → Sm F → Sm G → Crystal	(compound with carbon numbers 11 and 12)

It is clearly evident from the above phase sequences that new smectic phases have been induced compared to pure benzoic acid homologous series. In other words, nematic and smectic C have been quenched and smectic G and smectic F phases are induced in the lower compounds of the homologous series, similar to how the higher mesogens of the series smectic C and nematic appeared in addition to the other smectic phases. Thus, a good number of mesogenic phases have been induced in the lower and higher mesogens of the present series.

DSC Studies

DSC thermograms were obtained in heating and cooling cycles. The sample was heated with a scan rate of 10°C/min and held at its isotropic temperature for one

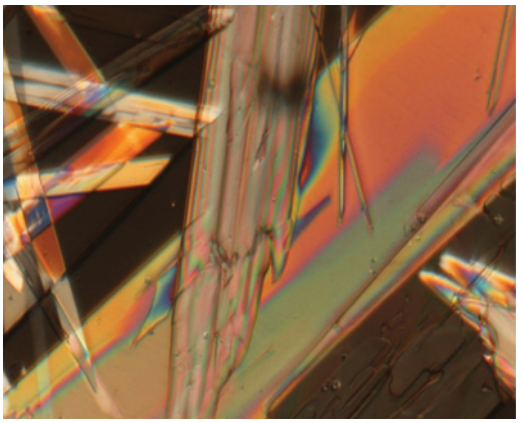

Figure 4. Smooth, multicolored mosaic texture of the smectic G phase.

minute to attain thermal stability. The cooling run was performed with a scan rate of 10 °C/min. The respective equilibrium transition temperatures and corresponding enthalpy values of the mesogens corresponding to the homologous series are listed separately in Table 1.

As a representative case, the phase transition temperatures and enthalpy values of nonyloxybenzoic acid compound (12A+9BA) (Figure 5) are discussed. As shown in Figure 5, in the cooling run, the DSC thermogram exhibited four distinct transitions, namely, isotropic to nematic, nematic to smectic C, smectic C to smectic F, and smectic F to crystal with transition temperatures 138.5°C, 112.6°C, 89.6°C, and 66.8°C with corresponding enthalpy values 3.10, 2.14, 28.76, and 71.07 J/g. In the heating cycle, three distant transitions, namely, crystal to melt, melt to nematic, and nematic to smectic C, were observed at 94.2°C, 141.8°C, and 116.2°C with corresponding enthalpy values 108.27, 3.36, and 3.93 J/g. These transition temperatures and corresponding thermal spans of individual phases concur with polarizing optical microscopy (POM) studies.

Phase Diagrams

Phase Diagram of Pure p-n-Alkyloxy Benzoic Acids. The phase diagrams of pure p-n-alkyloxy benzoic acids and the dodecyl aniline homologous series were constructed through POM studies by the phase transition temperatures observed in the cooling run of the mesogens of the present homologous series. The phase diagram of pure p-n-alkyloxy benzoic acids is shown as Figure 6a. Transition temperatures are plotted against the alkyloxy carbon number pertaining to the alkyloxy benzoic acids. In the phase diagram, the transition temperatures obtained by DSC in cooling run are plotted on the x-axis and the alkyloxy carbon number of the benzoic acid is shown on the y-axis. The isotropic temperatures of all of the members of the homologous series formed an upper boundary of the phase diagram and the crystallization temperatures formed the lower boundary. In between these two boundaries all the other phases exhibited by the homologous series is presented. The envelope of all phase transition temperatures corresponding

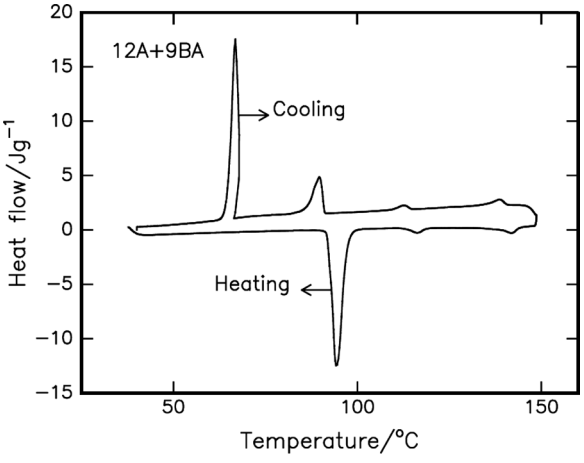

Figure 5. DSC thermogram of 12A+9BA.

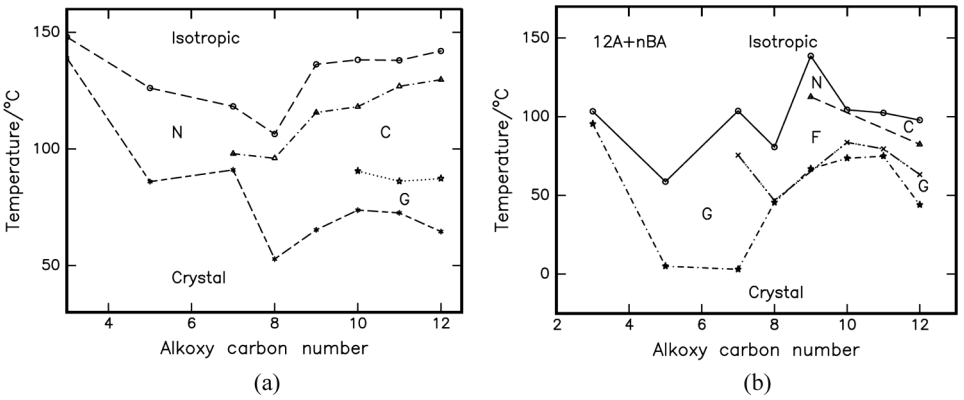

Figure 6. (a) Phase diagram of pure p-n-alkyloxy benzoic acids. (b) Phase diagram of dodecylaniline and alkyloxy benzoic acid hydrogen-bonded series.

to the same phase in various members of the same homologous series is connected by a line. Such a phase diagram for the present homologous series was constructed and the following points can be observed from Figure 6a:

(a) As the alkyloxy carbon number increased it was found that the mesogenic thermal range also increased and the phase polymorphism (nematic, smectic C and G) was observed.
(b) The nematic phase was observed in all the members of the alkyloxy benzoic acid homologous series.
(c) A tilted phase, namely, smectic C, was induced from heptyloxy benzoic acid.
(d) Another higher ordered phase, namely, smectic G, was induced from decyloxy benzoic acid, quenching the ranges of nematic and smectic C phases.
(e) The odd–even effect is not pronounced, either in the isotropic end or in the crystalline end.
(f) In the entire homologous series the crystalline temperatures were found to fall from ~148°C in butyloxy benzoic acid to ~60°C in dodecyloxy benzoic acid

Phase Diagram of Homologous Series (12A +nBA) Complex. The phase diagram of dodecyl aniline with p-n-alkyloxy benzoic acids is depicted in Figure 6b. A careful observation of Figure 6b reveals the following points:

(a) The members of the homologous series exhibit nematic, smectic C, smectic F, and smectic G phases.
(b) A noteworthy point of the present homologous series is two lower order mesogens, namely, pentyloxy benzoic acid (12A+5BA) and heptyloxy benzoic acid (12A+7BA) compounds, which exhibited smectic G ordering far below room temperature (~3°C to 5°C).
(c) It was observed that as the alkyloxy carbon number increased the mesogenic polymorphism increased. In other words, the propyloxy benzoic acid compound exhibited only one phase (smectic G) and the dodecyloxy benzoic acid compound possessed three phases (smetic C, smetic F, and smetic G).
(d) Smectic F and smectic G phases were induced in the lower order mesogens (propyloxy to octyloxy) of homologous series, whereas the pure alkyloxy

benzoic acid showed nematic and smectic C phases. Thus, in the present homologous series nematic and smectic C phases were quenched with the onset of new phases smectic F and Smectic G.

(e) In the higher order of the homologous series from nonyloxy to dodecyloxy benzoic acid compounds, smectic C, smectic F, and smectic G phases were observed. Thus, when compared to the pure alkyloxy benzoic acid, nematic and smectic C were quenched.
(f) Interestingly, the odd–even effect was visible in the isotropic transitions but suppressed at crystal transition temperatures.
(g) In summary, it can be concluded that in the present series crystallization temperatures fall far below those of pure alkyloxy benzoic acid (Figures 6a and 6b).

Influence of Alkyloxy Carbon Number

From Figures 6a and 6b it can be inferred that alkyloxy carbon chain length has a pronounced effect on the phase variance, mesogenic thermal span, and favored phase. In other words, as the alkyloxy carbon number increased the following facts were noticed:

(a) In the present homologous series the crystallization temperatures of all of the mesogens were observed to be below 100°C.
(b) The first mesogen of the series, that is, 12A+3BA, showed smectic G phase, whereas the last mesogen of the series, that is, 12A+12BA, was found to exhibit smectic C, smectic F, and smectic G phases. Thus, as the alkyloxy carbon increased, the mesogenic polymorphism progressively increased.
(c) The overall mesogenic range increased drastically from ~8°C in the 12A+3BA mesogen to ~54°C in 12A+12BA mesogen. Thus, the increment of the carbon number favored an increment in the mesogenic thermal range.

Role of Hydrogen and Oxygen toward Liquid-Crystalline Polymorphism. It is well known [21] that hydrogen bonding can affect the chain length, chain packing rigidity, and molecular order. Further, hetero intermolecular hydrogen-bonded networks favor [21] smectic phases through self-assembly of the molecules in liquid-crystalline compounds.

Reported studies [22–26] on Schiff's base liquid-crystalline compounds (N-(p-n-alkyloxy benzylidene)-p-alkylaniline), (N-(p-n-alkylbenzylidene)-p-alkyloxylaniline), and (N-(p-n-alkylbenzylidene)-p-alkylaniline) (designated as nO.m, n.Om, and n.m) suggest that the phase polymorphism is solely due to the positional presence of an electronegative oxygen atom in the rod-like molecule. Oxygen plays a pivotal role in favoring the liquid-crystalline phases, in particular the smectic ordering. Removal of oxygen in Schiff's base liquid-crystalline compounds resulted [22] in loss of liquid crystallinity. On the other hand, shifting the position of oxygen in the molecular network favored the abundance and evolution of new phases.

In the present study of 12A+nBA intra-hydrogen-bonded compounds, there is a head-to-head hydrogen-bonding interaction between centro-symmetrically related carboxyl groups in the monomer. This results in the formation of a dimer. It is reported [6] that this type of interaction favors the smectic ordering to be exhibited and at the same time fully validates geometric estimations based on theoretical calculations.

Possibilities to change the molecular arrangement of hydrogen-bonded dimers of carboxylic acids by offering other acceptor groups are reported [27] in different

species of molecules, namely, in amino acid conjugates, in sulfinyl and phosphinyl-carboxylic acids, and in some p-n-alkyloxy benzoic acids. As a result, it was found [27] that the carboxylic dimers are rather easily broken by lattice forces, by forming other intra- and intermolecular hydrogen bonds to stronger acceptor groups and by increasing the temperature. This result concurs with the present observation of higher isotropic temperatures observed in the present hydrogen-bonded compound.

Thus, it may be argued that the addition of the phases in the 12A+nBA series is due to the presence and position of electronegative-rich oxygen, which is situated at the hydrogen-bonded sites and at the benzoic acid terminal.

Dielectric Studies

Dielectric studies enable detection of a second-order transition that was unobserved in the DSC study. Variation of capacitance and dielectric loss with temperature was performed for all of the members of the present homologous series. The mesogen filled in a conducting cell was excited with a frequency of 100 KHz. Simultaneous textural observations were made to corelate the phase exhibited by the mesogen. Thus, the textural transition temperatures and dielectric spectrum were studied together.

As a representative case, the dielectric spectrum of undecyloxy benzoic acid compound (12A+11BA) as depicted in figure 7 is discussed below. From Figure 7 the following points can be inferred:

(a) As the temperature is decreased from isotropic, a peak is observed at 89°C, indicating the onset of the smectic C phase. A Schlieren texture was observed, indicating the smectic C phase.
(b) On further decrement of the temperature, stabilization of the smectic C phase was evinced where the permittivity started increasing without any sudden anomaly in the dielectric spectrum.
(c) At 81.3°C a sudden decrement in the permittivity magnitude indicated the onset of the smectic F phase. A checkerboard texture was observed with the onset of the smectic F phase.

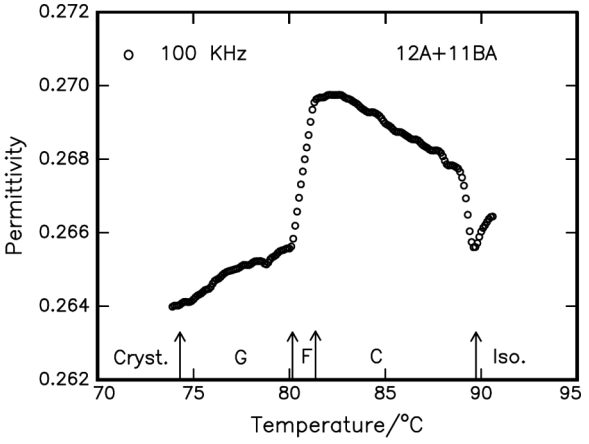

Figure 7. Permittivity variance with temperature of 12A+11BA at 100 KHz.

(d) A smectic G phase texture was observed and in the dielectric spectrum a sudden steep fall in the magnitude of permittivity at 80.1°C indicated the transition from a smectic F phase to a smectic G phase. A smooth, multicolored mosaic texture was observed, indicating the onset of the smectic G phase.
(e) A further decrement in temperature showed an unaltered variation of the permittivity indicating stabilization of the smectic G phase.
(f) A small variation in the magnitude of the permittivity at 74.7°C was attributed to the transition from the mesogenic phase to crystal. The formation of crystals, was also evinced through optical textural studies.

Dielectric Relaxation Studies

The dielectric dispersion, viz. $\varepsilon''(\omega)$ and $\varepsilon'(\omega)$ studied at different temperatures in the smectic C phase of various hydrogen-bonded compounds appears to be asymmetric about ε'' (maximum). Such asymmetric non-Debyes-type of off-centered dispersion is studied by Cole-Davidson theory [28–30] and is given by

$$\varepsilon''(\omega) = \{\varepsilon_\infty - [(\Delta\varepsilon)]/[1 + (j\omega\tau)^{1-\alpha}]\}$$

where $\Delta\varepsilon = (\varepsilon_0 - \varepsilon_\infty)$ is the dielectric strength; $\omega = 2\pi f$, where f is the frequency of the ac signal; τ is relaxation time, that is, $1/f_r$, and α is the distribution parameter (or degrees of freedom) estimate the influence of the environment of dipole and its fixation (in molecular frame) during the reorientation.

Cole-Cole plots are constructed for various temperatures in the smectic C phase at different frequencies, with permittivity on the x-axis and dielectric loss on the y-axis. Figures 8 and 9 illustrate such a Cole-Cole plot in the smectic C phase and the Arrhenius graphs for the various hydrogen-bonded compounds, respectively. From these plots the f_r for various temperatures were experimentally determined and their activation energies are tabulated in Table 2.

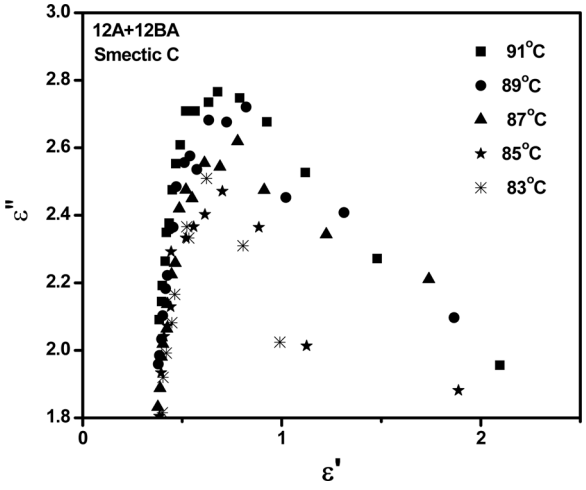

Figure 8. Cole-Cole plots of 12A+12BA at various temperatures.

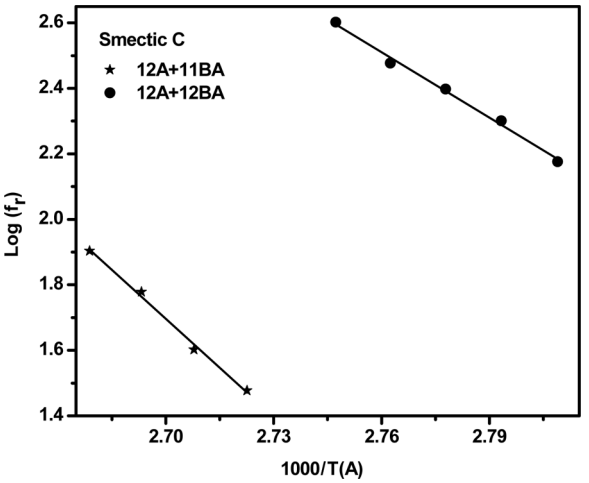

Figure 9. Arrhenius plots for 12A+12BA and 12A+11BA compounds.

Relaxations in 12A+12BA Compound. In the smectic C phase of 12A+12BA the dielectric relaxations were recorded at various temperatures, viz. 91°C, 89°C, 87°C, 85°C, and 83°C. Cole-Cole plots for the compound were constructed (Figure 8). The ε'' (maximum) represents the magnitude of the maximum dielectric loss recorded at a specific temperature for the compound. It has been observed that as the temperature increases, the magnitude of ε'' (maximum) varied from 2.766 to 2.471. Data of the magnitude of f_r for various temperatures are listed in Table 2. It can be noticed from Table 2 that at the onset of the smectic C phase, the magnitude of the relaxation frequency is maximum; as the temperature is incremented this magnitudes is observed to decrease until it reaches a saturated value at the end set of the smectic C transition. The relaxation frequency shifted from 400 to 150 Hz with the decrement of the temperature from 91°C to 83°C. From these data, Arrhenius plots are constructed as shown in Figure 9. It can be noticed that the magnitude of the relaxation frequency decreased with a decrement in the

Table 2. Relaxation frequency (f_r) at different temperatures for various hydrogen-bonded compounds in the smectic C phase

Complex	Temperature (°C)	Relaxation frequency (Hz)	$\varepsilon''_{(max)}$	Activation energy (eV)
12A+12BA	91.0	400	2.766	0.66
	89.0	300	2.721	
	87.0	250	2.619	
	85.0	200	2.509	
	83.0	150	2.471	
12A+11BA	100.3	80	10.754	0.99
	98.3	60	10.625	
	96.3	40	10.554	
	94.3	30	10.292	

temperature. Further, the activation energy in the smectic C phase was experimentally found to be 0.66 eV.

Relaxations in 12A+11BA Compound. In this compound, relaxations in the smectic C phase were carried out at four temperatures, viz. 100.3°C, 98.3°C, 96.3°C, and 94.3°C. With the decrement of temperature the relaxation frequency shifted from 80 to 30 Hz and the corresponding magnitude of ε'' (maximum) varied from 10.754 to 10.292. Various Cole-Cole plots were constructed and the f_r for various temperatures were experimentally determined and tabulated in Table 2. From the Arrhenius plots (Figure 9) the respective activation energy of this compound was calculated to be 0.99 eV.

Conclusions

1. A hydrogen bond was formed between p-n-alkyloxy benzoic acids (nABA) and dodecyl aniline. The resulting compounds were isolated and characterized.
2. The mesogens isolated were characterized by FTIR, DSC, dielectric, and POM studies.
3. Two mesogens, namely, petnyl and heptyl alkyloxy benzoic acid with dodecyl aniline, respectively exhibited, smectic G ordering far below ambient temperatures.

Acknowledgment

The authors acknowledge the financial support rendered by the All India Council of Technical Education (AICTE), Department of Science and Technology (DST), and Defence Research Development Organization (DRDO). Infrastructural support provided by the Bannari Amman Institute of Technology is gratefully acknowledged.

References

[1] Ishihara, S., Furuki, Y., & Takeoka, S. (2008). *Polymer. Adv. Tech.*, *19*, 1097.
[2] (a) Nguyen, H. L., Horton, P. N., Hursthouse, M. B., Legon, A. C., & Bruce, D. W. (2004). *J. Am. Chem. Soc.*, *16*, 126; (b) Metrangolo, P., Präsang, C., Resnati, G., Liantonio, R., Whitwood, A. C., & Bruce, D. W. (2006). *Chem. Comm.*, 3290.
[3] Prasang, C., Whitwood, A. C., & Bruce, D. W. (2008). *Chem. Comm.*, 2137; (b) Fox, D., Metrangolo, P., Pasini, D., Pilati, T., Resnati, G., & Terraneo, G. (2008). *Cryst. Eng. Comm.*, *10*, 1132.
[4] (a) Toh, C. L., Xu, J., Lu, X., & He, C. (2008). *Liq. Cryst.*, *35*, 241; (b) Kutsumizu, S., Mori, H., Fukatami, M., Naito, S., Sakajiri, K., & Saito, K. (2008). *Chem. Mater.*, *20*, 3675.
[5] (a) Wojciech, P., Zeijko, T., Martin, W., Robert, G., Maarten, J. P., Meijer, E. W., & Albertus, P. H. J. S. (2008). *J. Mat. Chem.*, *18*, 2968; (b) Ozawa, K., Yamamura, Y., Yasuzuka, S., Mori, H., Kutsumizu, S., & Saito, K. (2008). *J. Phys. Chem. B*, *112*, 12179.
[6] (a) Sreedevi, B., Chalapathi, P. V., Kotikalapudi, V. K. M., Pisipati, V. G. K. M., & Potukuchi, D. M. (2007). *Ferroelectrics*, *18*, 361; (b) Montani, R. S., Garay, R. O., Cukiernik, F. D., Garland, M. T., & Baggio, R. (2009). *Acta Cryst. C*, *56*, 81.
[7] Letellier, P., Ewing, D. F., Goodby, J. W., Haley, J., Kelly, S. M., & Mackenzie, G. (1997). *Liq. Cryst.*, *22*, 609.
[8] Kumar, P. A., Srinivasulu, M., & Pisipati, V. G. K. M. (1999). *Liq. Cryst.*, *26*, 1339.
[9] Rudquist, P., Korblova, E., Walba, D. M., Shao, R., Clark, N. A., & Maclennan, J. E. (1999). *Liq. Cryst.*, *26*, 1555.

[10] Srinivasulu, M., Satyanarayana, P. V. V., Kumar, P. A., & Pisipati, V. G. K. M. (2001). *Liq. Cryst.*, *28*, 1321.
[11] Barmatov, E. G., Bobrovsky, A. Yu., Barmatova, M. V., & Shibaev, V. P. (1999). *Liq. Cryst.*, *26*, 581.
[12] Sideratov, Z., Tsiourvas, D., Paleos, C. M., & Skoulios, A. (1997). *Liq. Cryst.*, *22*, 51.
[13] Kato, T., & Frechet, J. M. J. (1989). *J. Am. Chem. Soc.*, *111*, 8533.
[14] Chitravel, T., Madhu Mohan, M. L. N., & Krishnakumar, V. (2008). *Mol. Cryst. Liq. Cryst.*, *493*, 17.
[15] Pisipati, V. G. K. M., Kumar, P. A., & Madhu Mohan, M. L. N. (2000). *Mol. Cryst. Liq. Cryst.*, *350*, 141.
[16] Madhu Mohan, M. L. N., Kumar, P. A., & Pisipati, V. G. K. M. (2001). *Mol. Cryst. Liq. Cryst.*, *366*, 431.
[17] (a) Vijayakumar, V. N., Murugadass, K., & Madhu Mohan, M. L. N. (2009). *Mol. Cryst. Liq. Cryst.*, *517*, 41; (b) Vijayakumar, V. N., Murugadass, K., & Madhu Mohan, M. L. N. (2009). *Mol. Cryst. Liq. Cryst.*, *515*, 37.
[18] Nakamoto, K. (1978). *Infrared and Raman Spectra of Inorganic and Co-ordination Compounds*, Wiley Interscience: New York.
[19] Swathi, P., Kumar, P. A., & Pisipati, V. G. K. M. (2000). *Liq. Cryst.*, *27*, 665.
[20] Gray, G. W., & Goodby, J. W. G. (1984). *Smectic Liquid Crystals: Textures and Structures*, Leonard Hill: London.
[21] Pillai, C. K. S., Sandhya, K. Y., Sudha, J. D., & Saminathan, M. (2003). *Pramana*, *61*, 417.
[22] Ajeetha, N., & Pisipati, V. G. K. M. (2003). *Z. Naturforsch.*, *58A*, 735.
[23] Rao, N. V. S., Potukuchi, D. M., & Pisipati, V. G. K. M. (1991). *Mol. Cryst. Liq. Cryst.*, *196*, 71.
[24] Kumar, P. A., Pisupati, S., Pisipati, V. G. K. M., Srinivasulu, Ch., & Narayana Murthy, P. (2002). *Liq. Cryst.*, *29*, 967.
[25] Alapati, P. R., Rao, N. V. S., Potukuchi, D. M., Pisipati, V. G. K. M., Paranjpe, A. S., & Rao, U. R. K. (1988). *Liq. Cryst.*, *3*, 1461.
[26] Potukuchi, D. M., Padmaja Rani, G., Srinivasulu, M., & Pisipati, V. G. K. M. (1998). *Mol. Cryst. Liq. Cryst.*, *319*, 19.
[27] Kolbe, A., Plass, M., Kresse, H., Kolbe, A., Drabowicz, J., & Zurawinski, R. (1997). *J. Mol. Struct.*, *436*, 161.
[28] Kobayashi, S., & Ishibashi, S. (1994). *Mol. Cryst. Liq. Cryst.*, *257*, 181.
[29] Jong-Guang, W., & Shu-Hsia, C. (1994). *Jpn. J. Appl. Phys.*, *33*, 6249.
[30] Qian, T., & Taylor, P. L. (1999). *Phys. Rev. E*, *60*, 2978.